PHYSICAL REVIEW B **96**, 035442 (2017)

Semiclassics for matrix Hamiltonians: The Gutzwiller trace formula with applications to graphene-type systems

M. Vogl,[*] O. Pankratov, and S. Shallcross

Lehrstuhl für Theoretische Festkörperphysik, Staudtstrasse 7-B2, 91058 Erlangen, Germany

(Received 28 November 2016; revised manuscript received 1 June 2017; published 27 July 2017)

We present a tractable and physically transparent semiclassical theory of matrix-valued Hamiltonians, i.e., those that describe quantum systems with internal degrees of freedoms, based on a generalization of the Gutzwiller trace formula for a $n \times n$ dimensional Hamiltonian $H(\hat{\mathbf{p}},\hat{\mathbf{q}})$. The classical dynamics is governed by n Hamilton-Jacobi (HJ) equations that act in a phase space endowed with a classical Berry curvature encoding anholonomy in the parallel transport of the eigenvectors of $H(\mathbf{p},\mathbf{q})$; these vectors describe the internal structure of the semiclassical particles. At the $\mathcal{O}(\hbar^1)$ level and for nondegenerate HJ systems, this curvature results in an additional semiclassical phase composed of (i) a Berry phase and (ii) a dynamical phase resulting from the classical particles "moving through the Berry curvature". We show that the dynamical part of this semiclassical phase will, generally, be zero only for the case in which the Berry phase is topological (i.e., depends only on the winding number). We illustrate the method by calculating the Landau spectrum for monolayer graphene, the four-band model of AB bilayer graphene, and for a more complicated matrix Hamiltonian describing the silicene band structure. Finally, we apply our method to an inhomogeneous system consisting of a strain engineered one-dimensional moiré in bilayer graphene, finding localized states near the Dirac point that arise from electron trapping in a semiclassical moiré potential. The semiclassical density of states of these localized states we show to be in perfect agreement with an exact quantum mechanical calculation of the density of states.

DOI: 10.1103/PhysRevB.96.035442

I. INTRODUCTION

In the $\hbar \to 0$ limit, the behavior of quantum systems can be expressed in terms of the classical phase space trajectories. For one-dimensional scalar problems, the Wentzel–Kramers–Brillouin (WKB) method [1–3] yields semiclassical wave functions and energy levels, an approach that can be generalized to both integrable multidimensional systems (Einstein–Brillouin–Keller (EBK) torus quantization [4]), as well as to systems with multicomponent wave functions [5–16]. In the latter case, however, the multicomponent wave function matching inherent in the WKB approach rapidly becomes prohibitively cumbersome as the number of components increases.

The Gutzwiller trace formula circumvents this matching problem by giving a direct expression for the semiclassical density of states. Furthermore, it is valid for systems with a nonintegrable (i.e., chaotic) classical limit. While generalizations of the trace formula for the multicomponent case have been presented for specific matrix Hamiltonians such as the relativistic Dirac Hamiltonian [17–22] and the Dirac-Weyl Hamiltonian of graphene [23,24], a general multicomponent version of the trace formula has not been considered. In the solid-state theory context, however, a semiclassical method applicable to *arbitrary matrix Hamiltonians* would be extremely useful. This is so for two reasons. First, in many systems, for instance, few-layer graphenes, topological insulators, and semiconductors, one encounters multiband effective Hamiltonians and hence multicomponent wave functions. Second, and perhaps most important, in the emerging class of low-dimensional materials one very often encounters structural deformations occurring on length scales far in excess of the lattice constant. Such deformations are very difficult to treat fully quantum mechanically (due to the huge unit cell sizes involved) while at the same time present a natural case for a semiclassical treatment (due to the slowly varying spatial deformation). Examples include flexural ripples in graphene [25], rotational stacking faults in few-layer graphene systems [26–29], the recently discovered partial dislocation networks in few-layer graphenes [30–32], and graphene nanostructures for which interesting semiclassical work already exists [33]. A general semiclassical approach for treating such systems thus has the potential of providing a very useful investigative tool.

The purpose of the present paper is therefore twofold: (i) to generalize the Gutzwiller trace formula to the case of arbitrary matrix-valued Hamiltonians and (ii) to demonstrate that the semiclassical approach yields an *accurate and tractable* scheme for the treatment of deformations in graphene-based systems. To that end, we will first focus on fundamental theory and some simple applications and in the final part of the paper consider application of the theory to a realistically complex example of a deformation in bilayer graphene, a one-dimensional strain moiré.

Let us briefly outline the differences between the matrix-valued case and the scalar case within a semiclassical treatment. At $\mathcal{O}(\hbar^0)$, a scalar Schrödinger equation reduces to the Hamilton-Jacobi equation of classical mechanics. For a $n \times n$ Hamiltonian, however, there are two important differences in the $\mathcal{O}(\hbar^0)$ classical structures. First, we obtain n Hamilton-Jacobi equations, some of which may be identical. This situation arises, for instance, in the $\hbar \to 0$ limit of the Dirac equation [17], where each of the two Hamilton-Jacobi equations (for particles and antiparticles) is twice degenerate; in the limit $\hbar \to 0$ there is no spin and hence one obtains two pairs of degenerate equations. As for the case of ordinary perturbation theory, such degenerate cases require a special

---

[*] Present address: Department of Physics, The University of Texas at Austin, Austin, TX 78712, USA.

treatment. Second, in contrast to the scalar case, for multiband quantum Hamiltonians the semiclassical particle types have internal structure (pseudospin structure in the case of graphene, for example) which is carried by the classical eigenvectors of $H(\mathbf{p},\mathbf{q})$. Anholonomy in the parallel transport of these eigenvectors then endows the corresponding Hamiltonian phase spaces with a classical $\mathcal{O}(\hbar^0)$ Berry curvature.

At $\mathcal{O}(\hbar)$ we obtain an equation for the amplitude that is transported along the classical orbits described by the Hamilton-Jacobi equations of motion. In contrast to the scalar case, for a matrix Hamiltonian this amplitude acquires an addition phase structure [6–9,34,35] from the $\mathcal{O}(\hbar^0)$ Berry curvature which for the *nondegenerate case* consists of (i) a geometrical phase and (ii) a dynamical phase that represents a record of the semiclassical particle moving through the Berry curvature, expressed via a (weighted) line integral over the particle orbit of a contraction between the Berry curvature and the symplectic matrix. The degenerate case does not permit this intuitive interpretation (however, see Ref. [34] for a geometric interpretation). In this case, one has a $U(N)$ rather than scalar Berry curvature, and the concomitant different time noncommutation precludes the expression of the semiclassical phase as a simple time integral.

Our approach differs from that taken by Carmier and Ullmo [23] in their semiclassical study of graphene and two-band bilayer graphene in that their description begins with the energy-dependent Green's function, which then enforces a complex matching procedure for the initial condition of this function; as in the case of the WKB method, this becomes prohibitively cumbersome for a general matrix - valued Hamiltonian. Following Bolte and Keppeler [17], we implement the initial conditions for the Green's functions at the level of the time-dependent Green's functions, which allows for an elegant solution that entirely circumvents the initial matching problem.

The procedure leading from an arbitrary matrix-valued Hamiltonian to the density of states is presented as an explicit set of steps, and we apply it to a number of cases where the exact solution is known: the Landau spectra of graphene, a four-band model of bilayer graphene, and silicene. As one would expect, the agreement between the exact and the semiclassical results becomes considerably degraded at low energies, and in particular for bilayer graphene the zero mode found in the exact solution is not captured within the semiclassical approximation (and is, of course, also not captured in the two-band approximation to this problem [23]). It is therefore by no means obvious that a semiclassical approach is suitable for graphene-based systems with slowly spatial deformations, as one is always interested in the low-energy behavior.

To explore this situation more closely, we consider a realistic example of such a deformation: a one-dimensional strain moiré in bilayer graphene, which serves as an instructive analog of the graphene twist bilayer [36], two mutually rotated layers of graphene. The twist bilayer displays extraordinarily rich electronic structure in small angle limit [26–29,37,38] (i.e., as the moiré length becomes large), and in particular a strong electron localization on the AA stacked regions of the lattice. We present an analytical semiclassical analysis of the strain moiré, finding that (i) at the Dirac point the action is orders of magnitude larger than $\hbar$ when the moiré length becomes large compared to the lattice constant—thus validating the semiclassical approach—and (ii) that the electron localization is driven by the existence of a *semiclassical potential well* centered at the AA spots that arises from the stacking potential in the quantum Hamiltonian. We should stress that this "potential well" picture, which provides a very natural description of charge localization, is fundamentally semiclassical: No such potential well could localize quantum mechanically due to the Klein paradox which prevents localization of electrons in graphene by a scalar potential. We furthermore find an analytical form for the semiclassical density of states arising from electrons trapped in this potential well, which we show to be in almost perfect agreement with exact quantum mechanical calculations. This demonstrates both that the semiclassical approach provides a valid tool for investigating slow deformations in few-layer systems, as well as the insight it can bring into the physics of these rather complex systems. It should be stressed that treating such a system on the basis of either the standard WKB approach (in principle possible as we have an effective one-dimensional system) or that of Ref. [23] could not be contemplated due to the extraordinarily complexity of the matching procedure that would be involved.

II. SEMICLASSICS FOR MATRIX-VALUED HAMILTONIANS

We consider Schrödinger's equation for the Green's function $G(\mathbf{r},\mathbf{r}',t)$ with a *matrix-valued* Hamiltonian $\hat{H}$

$$i\hbar\partial_t G(\mathbf{r},\mathbf{r}',t) = \hat{H}(-i\hbar\partial_i,x_i)G(\mathbf{r},\mathbf{r}',t) \tag{1}$$

and the initial condition

$$G(\mathbf{r},\mathbf{r}',0) = \mathbb{1}_n\delta(\mathbf{r}-\mathbf{r}'). \tag{2}$$

We will assume that the elements of $H(\mathbf{p},\mathbf{q})$ are smooth functions and introduce the following convention: The *primed* coordinates are *initial* coordinates with the *nonprimed* ones the *final* coordinates on a classical trajectory.

Let us first derive an expression for the time-dependent Green's function using a generalization of the ansatz provided by Bolte and Keppeler [17]. If $\hat{H}$ is a $n \times n$ matrix, we search for the *time-dependent Green's function* of the form

$$\begin{aligned} G(\mathbf{r},\mathbf{r}',t) = {} & \frac{1}{(2\pi\hbar)^d}\int d^dp' \sum_\alpha \hat{V}_\alpha(t,\mathbf{r},\mathbf{p}') \\ & \times \hat{f}_\alpha(t,\mathbf{r},\mathbf{r}',\mathbf{p}')\hat{V}_\alpha^\dagger(0,\mathbf{r}',\mathbf{p}')e^{\frac{i}{\hbar}\Phi_\alpha(\mathbf{r},\mathbf{r}',\mathbf{p}',t)}. \end{aligned} \tag{3}$$

This ansatz is completely general and could describe the exact solution to Eq. (1); however, the $e^{\frac{i}{\hbar}\Phi_\alpha(\mathbf{r},\mathbf{r}',\mathbf{p}',t)}$ term allows a WKB-like expansion in orders of $\hbar$ and, due to the integral in Eq. (3), one can implement the initial condition Eq. (2) by requiring

$$\begin{aligned} \hat{f}_\alpha(t=0) &= 1, \\ \Phi_\alpha(t=0) &= \mathbf{p}'(\mathbf{r}-\mathbf{r}'), \\ \sum_\alpha \hat{V}_\alpha(0,\mathbf{r}',\mathbf{p}')V_\alpha^\dagger(0,\mathbf{r}',\mathbf{p}') &= \mathbb{1}_n. \end{aligned} \tag{4}$$

We now assume that $\hat{V}_\alpha = \hat{V}_\alpha^{(0)} + \hbar\hat{V}_\alpha^{(1)} + \cdots$ is analytical in $\hbar$ (a similar $\hbar$ expansion will hold for the f_α) and insert Eq. (3)

into the Schrödinger equation Eq. (1) and collect terms of $\mathcal{O}(\hbar^0)$. This procedure leads to the *zero eigenvalue condition*

$$[H(\partial_\mu \Phi_\alpha, x_i) + \partial_t \Phi_\alpha]\hat{V}_\alpha^{(0)} = 0. \tag{5}$$

[We may drop the sum and integral in Eq. (3) as the equation is linear.] There are evidently n solutions to this equation which occur when the $\hat{V}_\alpha^{(0)}$ are equal to the n orthonormal eigenvectors of $H(\partial_\mu \Phi_\alpha, x_i)$. Denoting the corresponding eigenvalue by H_α, we find that the zero eigenvalue equation implies the existence of n Hamilton-Jacobi equations

$$H_\alpha = -\partial_t \Phi_\alpha, \tag{6}$$

from which we then immediately identify for system α the following objects: H_α is a classical scalar Hamiltonian, the real scalar function $\Phi_\alpha(\mathbf{r},\mathbf{r}',\mathbf{p}',t)$ is a classical action, and $p_\mu^\alpha = \partial_\mu \Phi_\alpha$ is the corresponding canonical momentum. Thus, a general $n \times n$ quantum Hamiltonian leads to n separate classical systems at order $\mathcal{O}(\hbar^0)$. The full classical information is contained in the n Hamilton-Jacobi equations (6) and the n vectors $\hat{V}_\alpha^{(0)}$.

The situation becomes more complicated if the matrix $H(p_i, x_i)$ has degenerate eigenvalues. In this circumstance, recourse to degenerate perturbation theory may be circumvented following the scheme of Bolte and Keppeler, in which the m_α orthogonalized eigenvectors corresponding to the degenerate eigenfunction H_α are combined into an $m_\alpha \times n$ full degenerate eigenvector that evidently satisfies $\hat{V}_\alpha^{(0)\dagger} H(p_i, x_i)\hat{V}_\alpha^{(0)} = H_\alpha \mathbb{1}_{m_\alpha}$. With the initial conditions

$$\begin{aligned} \hat{f}_\alpha(t=0) &= \mathbb{1}_m, \\ \Phi_\alpha(t=0) &= \mathbf{p}'(\mathbf{r}-\mathbf{r}'), \\ \sum_\alpha \hat{V}_\alpha(0,\mathbf{r}',\mathbf{p}')\hat{V}_\alpha^\dagger(0,\mathbf{r}',\mathbf{p}') &= \mathbb{1}_n, \end{aligned} \tag{7}$$

the initial condition of the Green's function equation is satisfied and the calculations thereafter proceed in a formally identical way for both the degenerate and nondegenerate cases, with the difference of course that the rank of the various objects in the theory differs between the two cases.

We now consider the $\mathcal{O}(\hbar)$ corrections to the n Hamilton-Jacobi equations, sewing "quantum flesh on classical bones", to use the evocative phrase of Berry and Mount [39]. The derivative operators $-i\hbar\partial_i$ in $\hat{H}_D$ are substituted by the canonical momenta p_μ^α upon acting on $e^{\frac{i}{\hbar}\Phi_\alpha}$. To generate the $\mathcal{O}(\hbar)$ terms from $\hat{H}_D$ we should allow every matrix element $[\hat{H}_D]_{ij}$ to act on the exponential until only first-order operator terms remain. For example, the term $i\hbar^3\partial_i\partial_j\partial_k$ would generate $-i\hbar p_{i\alpha} p_{j,\alpha}\partial_k + (k \leftrightarrow j) + (k \leftrightarrow i)$. The resulting matrix operator $-i\hbar H_D^1$ is therefore linear in first-order derivatives. Considering $-i\hbar H_D^1$ as a perturbation, we obtain in first-order perturbation theory the $\mathcal{O}(\hbar)$ equation

$$\hat{V}_\alpha^{(0)\dagger}\big[H_D^1 + \partial_t\big]\hat{V}_\alpha^{(0)}\hat{f}_\alpha(\mathbf{r}) = 0, \tag{8}$$

which, as we shall now show, is a *transport equation* for $f_\alpha(\mathbf{r})$ along the classical trajectories governed by the H_α Hamiltonian. [Note that substitution of Eq. (3) into the Schrödinger equation Eq. (1), collecting terms of $\mathcal{O}(\hbar)$, and premultiplying by $V_\alpha^{(0)\dagger}$ also leads to Eq. (8).] In the case of degenerate Hamilton-Jacobi systems $f_\alpha(\mathbf{r})$ will be an $m_\alpha \times m_\alpha$ matrix; in the nondegenerate case $f_\alpha(\mathbf{r})$ is a scalar function.

To simplify the notation, we now define

$$\begin{aligned} H_{cl}(p_i, x_i) &:= H(p_i, x_i) + \partial_t \Phi_\alpha, \\ \lambda_\alpha &= \partial_t \Phi_\alpha + H_\alpha, \end{aligned} \tag{9}$$

such that Eqs. (5) and (6) take the form $H_{cl}\hat{V}_\alpha = 0$ and $\lambda_\alpha = 0$ respectively.

We now demonstrate that Eq. (8) may be written in the form of a transport equation familiar from the scalar case. We first note a rather obvious relation connecting H_D^1 and H_{cl}, namely,

$$\big[H_D^1\big]_{lm} = \sum_{k=1}^{d} \partial_{p_k}[H_{cl}]_{lm}\partial_k. \tag{10}$$

This identity follows from deployment of the Leibnitz rule on the right-hand side that generates all terms from $H(p_i, x_i)$ with one momentum variable removed and replaced by the operator ∂_k, exactly the definition of H_D^1 on the left-hand side. The identity Eq. (11) generalizes a similar relation used by Carmier and Ullmo [23] in their semiclassical treatment of single-layer graphene and the two-band model of bilayer graphene. In accordance with convention, we set $\partial_t = \partial_0$, $\partial_E = \partial_{p_0}$ and make use of the sum convention, letting the sum run from $\mu = 0, \ldots, d$, where d is the space dimension. We may then compactly write

$$H_D^1 + \partial_t = \partial_{p_\mu} H_{cl}\partial_\mu \tag{11}$$

and using this result can write Eq. (8) as

$$\big[\hat{V}_\alpha^{(0)\dagger}\big[\partial_{p_\mu} H_{cl}\big]\partial_\mu \hat{V}_\alpha^{(0)} + \hat{V}_\alpha^{(0)\dagger}\big[\partial_{p_\mu} H_{cl}\big]\hat{V}_\alpha^{(0)}\partial_\mu\big]\hat{f}_\alpha(\mathbf{r}) = 0. \tag{12}$$

Since we do not intend to calculate the higher order corrections to $\hat{V}_\alpha^{(0)}$ from now on we shall drop the index (0) at all vectors V_α.

We now we split $\hat{V}_\alpha^\dagger \partial_{p_\mu} H_{cl}\partial_\mu \hat{V}_\alpha$ into a Hermitian and an anti-Hermitian part. We denote the anti-Hermitian part iM_α:

$$iM_\alpha = \mathrm{Antiherm}\big(\hat{V}_\alpha^\dagger \partial_{p_\mu} H_{cl}\partial_\mu \hat{V}_\alpha\big). \tag{13}$$

(Note that in the case of an m_α-fold degeneracy M_α is a $m_\alpha \times m_\alpha$ matrix.) This term, as we will subsequently discuss in detail, results in an additional phase structure involving both a semiclassical analog of the Berry phase and a dynamical semiclassical phase that can be expressed in terms of the underlying Berry curvature.

By repeatedly applying the Leibnitz rule and using the fact that $\partial_{p_\mu} H_{cl}$ is Hermitian, we see that the Hermitian part of $\hat{V}_\alpha^\dagger \partial_{p_\mu} H_{cl}\partial_\mu \hat{V}_\alpha$ takes the following simple form:

$$\mathrm{Herm}\big(\hat{V}_\alpha^\dagger\big[\partial_{p_\mu} H_{cl}\big]\partial_\mu \hat{V}_\alpha\big) = \tfrac{1}{2}\partial_\mu\big(\partial_{p_\mu^\alpha}\lambda_\alpha\big) - \hat{\Lambda}_\alpha, \tag{14}$$

where we have also used the Hellmann-Feynman theorem $\hat{V}_\alpha^\dagger \partial_\gamma H_{cl} V_\alpha = \partial_\gamma \lambda_\alpha$ and the term

$$\hat{\Lambda}_\alpha = \tfrac{1}{2}\hat{V}_\alpha^\dagger \partial_\mu \partial_{p_\mu^\alpha}\hat{V}_\alpha \tag{15}$$

arises only in the case that the Hamiltonian has derivatives with position-dependent coefficients (for all the examples we consider here this will not be the case, although it will arise, for example, in the case of minimal coupling of a gauge field to quadratic momentum orders in the Hamiltonian). Applying the Hellmann-Feynman theorem to the second part of Eq. (12), we find that the equation simplifies to

$$\left[\frac{1}{2}\partial_\mu\left(\partial_{p^\alpha_\mu}\lambda_\alpha\right)+\left(\partial_{p^\alpha_\mu}\lambda_\alpha\right)\partial_\mu+iM_\alpha-\hat{\Lambda}_\alpha\right]\hat{f}_\alpha(\mathbf{r})=0. \tag{16}$$

From Hamilton's equations, we have $(\partial_{p^\alpha_\mu}\lambda_\alpha)=\dot{x}_\mu$ with $\dot{x}_0=1$ and so Eq. (16) reduces to the *transport equation*

$$\left[\frac{1}{2}\partial_\mu\left(\partial_{p^\alpha_\mu}\lambda_\alpha\right)+\frac{d}{dt}+iM_\alpha-\hat{\Lambda}_\alpha\right]\hat{f}_\alpha(\mathbf{r})=0, \tag{17}$$

which is similar to the scalar case but *with the additional matrices* M_α *and* $\hat{\Lambda}$. It should be stressed that M_α and $\hat{\Lambda}$ appear only for matrix-valued Hamiltonians. All terms in Eq. (17) are expressed in terms of the classical orbits obtained from the order $\mathcal{O}(\hbar^0)$ approximation.

Equation (17) must now be integrated along the classical orbits such that $f_\alpha(\mathbf{r})$ is "transported" along these orbits. The first two terms of this expression are scalars, and hence the ansatz $\hat{f}_\alpha=g_\alpha(\mathbf{r})\hat{h}_\alpha(\mathbf{r})$, where g_α is a scalar function that solves an auxiliary equation $[\frac{1}{2}\partial_\mu(\partial_{p^\alpha_\mu}\lambda_\alpha)+\frac{d}{dt}]g_\alpha(\mathbf{r})=0$, is sensible. The term $\hat{h}_\alpha(\mathbf{r})$ is an $m_\alpha\times m_\alpha$ matrix in the case of an m_α-fold degeneracy for H_α. The expression for $g_\alpha(\mathbf{r})$ with initial condition $g_\alpha(\mathbf{r})|_{t=0}=1$ is known from the scalar case (see, for example, Refs. [40,41]):

$$g_\alpha(\mathbf{r})=\sqrt{\det\left(\frac{\partial(\mathbf{p}_\alpha,t)}{\partial(\mathbf{p}',t)}\right)}. \tag{18}$$

Inserting $\hat{f}_\alpha=g_\alpha(\mathbf{r})\hat{h}_\alpha(\mathbf{r})$ into Eq. (17) yields

$$\left[\frac{d}{dt}+iM_\alpha-\hat{\Lambda}_\alpha\right]\hat{h}_\alpha(\mathbf{r})=0, \tag{19}$$

which is then solved by a *time-ordered exponential* (matrices M_α at different times will in general not commute).

We now have all ingredients required to calculate the time-dependent Green's function, Eq. (3). The remaining steps of the derivation now follow closely the scalar case, and we will, therefore, be brief in the presentation. From the initial condition Eq. (4) for the classical actions Φ_α it follows that $\Phi_\alpha=\phi_\alpha(\mathbf{r},\mathbf{p}',t)-\mathbf{p}'\mathbf{r}'$ [17], where ϕ_α are as yet unknown functions. We evaluate Eq. (3) with the stationary phase approximation to find

$$\begin{aligned}G(\mathbf{r},\mathbf{r}',t)\approx{}&\frac{1}{(2\pi i\hbar)^{\frac{d}{2}}}\sum_{\alpha,\gamma_t}g_{\alpha,\gamma_t}\hat{V}_{\alpha,\gamma_t}(\mathbf{r},t)\\&\times\hat{h}_{\alpha,\gamma_t}(\mathbf{r},\mathbf{r}',t)\hat{V}^\dagger_{\alpha,\gamma_t}(\mathbf{r}',0)e^{\frac{i}{\hbar}S_{\alpha,\gamma_t}(\mathbf{r},\mathbf{r}',t)-i\frac{\pi}{2}\nu_{\alpha,\gamma_t}}\end{aligned} \tag{20}$$

with

$$g_{\alpha,\gamma_t}=\sqrt{\left|-\det\left(\frac{\partial(\mathbf{p}_{\alpha,\gamma_t},t)}{\partial(\mathbf{r}',t)}\right)\right|}. \tag{21}$$

Here the stationary phase applied to the $\mathbf{p}'$ integral has enforced the sum over γ_t to be over all classical paths leading from $\mathbf{r}'$ to $\mathbf{r}$ within the time interval t. The actions $S_{\alpha,\gamma_t}(\mathbf{r},\mathbf{r}',t)$ are the classical actions that solve the Hamilton-Jacobi equations with this requirement. Additionally, ν_{α,γ_t} is the path-specific time-dependent Maslov index (or Morse index) that arises from taking the absolute value in the expression for g_{α,γ_t}. The Morse index accounts for the sign changes of the determinant under the square root, which occurs when the Lagrangian manifold corresponding to the dynamics of the Hamiltonian H_α develops a fold (see, for example, the book of Cvitanovic [42]). In a one-dimensional problem, this simply corresponds to the turning points of the classical path at which the Green's function picks up a phase $\frac{\pi}{2}$.

We now determine the retarded energy-dependent Green's function

$$G(\mathbf{r},\mathbf{r}',E)=\lim_{\epsilon\to0}\frac{1}{i\hbar}\int_0^\infty dt\,G(\mathbf{r},\mathbf{r}',t)e^{\frac{i}{\hbar}(E+i\epsilon)t} \tag{22}$$

within the stationary phase approximation. The calculation is again almost identical to the scalar case and we thus, for brevity of presentation, refer the reader to the standard literature for the scalar Gutzwiller formula (see, for example, Ref. [42]) and quote the result of the stationary phase approximation for the matrix valued case:

$$\begin{aligned}G(\mathbf{r},\mathbf{r}',E)\approx{}&\frac{1}{i\hbar(2\pi i\hbar)^{(d-1)/2}}\sum_{\alpha,\gamma_E}g_{\alpha,\gamma_E}\\&\times\hat{V}_{\alpha,\gamma_E}(\mathbf{r})\hat{h}_{\alpha,\gamma_E}(\mathbf{r},\mathbf{r}')\hat{V}^\dagger_{\alpha,\gamma_E}(\mathbf{r}')\\&\times e^{\frac{i}{\hbar}S_{\alpha,\gamma_E}(\mathbf{r},\mathbf{r}',E)-i\frac{\pi}{2}\nu_{\alpha,\gamma_E}},\end{aligned} \tag{23}$$

where

$$g_{\alpha,\gamma_E}=\sqrt{\left|-\frac{1}{\dot{r}^{\parallel}_{\alpha,\gamma_E},\dot{r}^{\parallel\prime}_{\alpha,\gamma_E}}\det\left(\frac{\partial^2S(\mathbf{r},\mathbf{r}',E)}{\partial\mathbf{r}^\perp\partial\mathbf{r}^{\perp\prime}}\right)\right|}, \tag{24}$$

and where the stationary phase condition now sets the summation to be on the *classical energy shell*. In this expression $S(\mathbf{r},\mathbf{r}',E)$ is now the energy-dependent action, and γ_E are all classical paths connecting $\mathbf{r}$ and $\mathbf{r}'$ at energy E. As is customary within a semiclassical formulation, we have chosen a coordinate system with one axis parallel ($\parallel$) to the trajectory and the other coordinates perpendicular ($\perp$) to the trajectory. Similar to Eq. (22), ν_{α,γ_E} is the *Maslov index* and counts the sign changes of the expression under the absolute value in g_{α,γ_E}.

We can now calculate the density of states simply by taking a trace over positions and over the matrix structure

$$d(E)=-\frac{1}{\pi}\lim_{\epsilon\to+0}\mathrm{Im}\{\mathrm{tr}[G(\mathbf{r},\mathbf{r}',E+i\epsilon)]\}. \tag{25}$$

The calculation of the position trace is, once again, identical to the scalar case which, following the standard procedure, evaluated in a stationary phase approximation for perpendicular coordinates and without any approximation (but assuming isolated orbits) for the parallel coordinates. This yields for the density of states

$$d_{\mathrm{osc}}(E)=\sum_{\alpha,\gamma_E^\circ}\mathrm{Im}\left[\frac{iT^p_{\alpha,\gamma_E^\circ}}{\hbar\pi}\mathrm{tr}(\hat{h}_{\alpha,\gamma_E^\circ})\frac{e^{\frac{i}{\hbar}S_{\alpha,\gamma_E^\circ}-i\frac{\pi}{2}\nu_{\alpha,\gamma_E^\circ}}}{\sqrt{\left|\det\left(\mathbb{J}_{\alpha,\gamma_E^\circ}-\mathbb{1}_{2(d-1)}\right)\right|}}\right], \tag{26}$$

where the position trace restricts the summation to the closed orbits, the stationary phase condition picks up only periodic orbits γ_E°, and the monodromy matrix $\mathbb{J}$ is given as

$$\mathbb{J}_{\alpha,\gamma_E^\circ} = \frac{\partial\big(p^\perp_{\alpha,\gamma_E^\circ},x^\perp_{\alpha,\gamma_E^\circ}\big)}{\partial\big(p^{\perp\prime}_{\alpha,\gamma_E^\circ},x^{\perp\prime}\big)}\bigg|_{(x^\perp_{\alpha,\gamma_E^\circ},p^\perp_{\alpha,\gamma_E^\circ})\in\gamma_E^\circ}, \tag{27}$$

which describes the stability of an orbit with respect to small deviations of the initial positions and momenta. It is evaluated for the orbit γ_E° and is independent of the point on the orbit which we choose for its evaluation [42]. The *Maslov index* is $\nu_{\alpha,\gamma_E^\circ}$ and it is important to note that, in general, it is not the same as the Maslov index in Eq. (24). For one-dimensional systems, however, these indices coincide. Lastly $T^p_{\alpha,\gamma_E^\circ}$ is the *time* needed to traverse the *primitive orbit* (primitive means traversing the orbit only once). Note that this result is valid only for the extended orbit contributions. For the short orbits, the exponential is not a fast oscillating function and the stationary phase approximation is inadmissible. Equation (26) provides the so-called oscillatory part of the density of states.

For the nondegenerate case, the M phase is a scalar, and thus Eq. (19) may be immediately solved to yield $h_{\alpha\gamma_E^\circ} = e^{-\int_0^{T_{\alpha,\gamma_E^\circ}} dt\,\Lambda_\alpha} e^{i\int_0^{T_{\alpha,\gamma_E^\circ}} dt\,M_\alpha}$, leading to a simpler Gutzwiller formula

$$d_{\rm osc}(E) = \sum_{\alpha,\gamma_E^\circ}\Bigg[\frac{T^p_{\alpha,\gamma_E^\circ}}{\hbar\pi}e^{-\int_0^{T_{\alpha,\gamma_E^\circ}} dt\,\Lambda_\alpha} \times \frac{\cos\big(\frac{1}{\hbar}S_{\alpha,\gamma_E^\circ} - \frac{\pi}{2}\nu_{\alpha,\gamma_E^\circ} + \int_0^{T_{\alpha,\gamma_E^\circ}} dt\,M_\alpha\big)}{\sqrt{\big|\det\big(\mathbb{J}_{\alpha,\gamma_E^\circ} - \mathbb{1}_{2(d-1)}\big)\big|}}\Bigg], \tag{28}$$

an expression that, in fact, differs from the scalar formula only by the addition of the M_α phase and the exponential term involving Λ_α that serves as an orbit weight function.

A. Relation between the semiclassical phase and the Berry phase

The existence of new phase structures associated with the short wavelength limit of multicomponent wave equations has a long history [5–9,34,35,43,44], including a curious anticipation of the geometric phase [43,44]. The phase structure of the semiclassical limit of multiband quantum Hamiltonians was first systematically addressed by Littlejohn and Flynn [7,8], following early work by Wilkinson and others [5,6,9], with the finding that the M_α phase consists of both a geometric as well as a dynamical part, with the latter phase more obscure in origin (described as the "no-name term" by Littlejohn and Flynn [8]).

Here we wish to show that the entire semiclassical phase can be understood in terms of an underlying Berry curvature, with, for the nondegenerate case, the second phase representing a dynamical record of the particle moving through the Berry curvature, expressed through an integral over the HJ orbit of a contraction between the curvature and the symplectic matrix (see, for example, Ref. [45] for the definition of the symplectic matrix). The existence of a dynamical phase associated with the Berry curvature is somewhat unusual and is a reflection of the fact that in the semiclassical theory we have a transport equation for the amplitude function f_α [Eq. (17)] and not the vectors V_α (which would simply be $\dot V_\alpha^\dagger V_\alpha = 0$ for parallel transport). For the degenerate case, this intuitive formulation of the semiclassical phase in terms of a geometric and dynamical part is not possible, due to the different time noncommutation of the corresponding $U(N)$ Berry curvature (see Ref. [34] for a geometric interpretation).

For the simpler nondegenerate case introducing the Berry curvature in this way lends, as we will show, considerable insight into the discussion of the semiclassical phase. For example, in the context of graphene-type systems, Carmier and Ullmo [23] have concluded that for Hamiltonians with no mass term, but arbitrary field $V(\mathbf{r})$, then the semiclassical phase is exactly the classical analog of the adiabatic Berry phase. This can be understood as a special case of the more general statement that if the Berry phase is topological (i.e., depends only on the winding number of the orbit) then the second semiclassical phase is zero. As we will show below, this more general statement follows very easily from consideration of the underlying Berry curvature.

The full form of this phase for the α HJ system is given by

$$\int_0^T dt\;M_\alpha = \int_0^T dt\;\Im V_\alpha^\dagger\big[\partial_{p_\mu}H_{cl}\big]\partial_\mu V_\alpha, \tag{29}$$

where for simplicity of notation we consider the case of nondegenerate Hamilton-Jacobi equations (the generalization is straightforward). Switching from four-vector notation to separate space and time derivatives we have for M_α

$$V_\alpha^\dagger\big[\partial_{p_\mu}H_{cl}\big]\partial_\mu V_\alpha = V_\alpha^\dagger\big[\partial_{p_i}H\big]\partial_i V_\alpha + V_\alpha^\dagger\partial_t V_\alpha. \tag{30}$$

If we insert into the right-hand side of this equation $H = \sum_\beta H_\beta V_\beta V_\beta^\dagger$ we then find for the integrand

$$\Im\left\{\dot x_\mu V_\alpha^\dagger\partial_i V_\alpha + V_\alpha^\dagger\partial_t V_\alpha + \sum_\beta H_\beta V_\alpha^\dagger\partial_{p_i}(V_\beta V_\beta^\dagger)\partial_i V_\alpha\right\}, \tag{31}$$

the first two terms of which are evidently the total time derivative $\Im V_\alpha^\dagger d_t V_\alpha$, i.e., represent a Berry phase that depends only on the geometry of the classical path. Using the notation $\mathbf{R} = (x_1,x_2,\ldots,x_d,p_1,p_2,\ldots,p_d)$ for a vector in a $2d$-dimensional phase space we write this as

$$\int_\Sigma \frac{1}{2}F_{\alpha\mu\nu}dR^\mu\wedge dR^\nu, \tag{32}$$

where $F_{\alpha\mu\nu} = \partial_\mu A_{\alpha\nu} - \partial_\nu A_{\alpha\mu}$ is the Berry curvature tensor, $A_{\alpha\mu} = iV_\alpha^\dagger\partial_\mu V_\alpha$ is the Berry connection for the α Hamilton-Jacobi system, and Σ is a hypersurface in the $2d$ Hamiltonian phase space. Note that the Greek indices μ, ν now run over the $2d$ dimensions of phase space in the vector $\mathbf{R}$.

What is the third term of Eq. (31)? Evaluation of the derivative $\partial_{p_i}(V_\beta V_\beta^\dagger)$ and insertion of the identity operator yields

$$\mathrm{Im}\sum_\beta(H_\beta - H_\alpha)\big(V_\alpha^\dagger\partial_{p_i}V_\beta\big)\big(V_\beta^\dagger\partial_i V_\alpha\big) \tag{33}$$

(note that the $\alpha = \beta$ term is identically zero in this sum). Using $\mathrm{Im}X = -i(X - X^*)/2$ we may write this as

$$-\frac{i}{2}\sum_\beta (H_\beta - H_\alpha)\big[\big(V_\alpha^\dagger \partial_{p_i} V_\beta\big)\big(V_\beta^\dagger \partial_i V_\alpha\big) - \big(V_\alpha^\dagger \partial_i V_\beta\big)\big(V_\beta^\dagger \partial_{p_i} V_\alpha\big)\big], \tag{34}$$

which has some resemblance to the antisymmetric structure of the Berry curvature tensor,

$$F_{\alpha\mu\nu} = i\sum_\beta [(V_\alpha^\dagger \partial_\nu V_\beta)(V_\beta^\dagger \partial_\mu V_\alpha) - (V_\alpha^\dagger \partial_\mu V_\beta)(V_\beta^\dagger \partial_\nu V_\alpha)]. \tag{35}$$

Equation (34), however, contains only terms diagonal in dimension and that have mixed p and x derivatives, while the curvature tensor contains all possible combinations of these indices. However, by contracting the curvature tensor with the symplectic matrix Ω we find

$$\frac{1}{4}\Omega^{\mu\nu}F_{\alpha\mu\nu} = \frac{i}{2}\sum_\beta \big[\big(V_\alpha^\dagger \partial_{p_i} V_\beta\big)\big(V_\beta^\dagger \partial_i V_\alpha\big) - \big(V_\alpha^\dagger \partial_i V_\beta\big)\big(V_\beta^\dagger \partial_{p_i} V_\alpha\big)\big], \tag{36}$$

which is, apart from the weight factor $(H_\beta - H_\alpha)$, identical to Eq. (34).

We may therefore express the semiclassical phase as

$$\int dt\, M_\alpha = \int_\Sigma \frac{1}{2}F_{\alpha\mu\nu}dR^\mu \wedge dR^\nu - \frac{1}{4}\int dt\, \sum_\beta \{H_\beta[\mathbf{R}(t)) - E]\Omega^{\mu\nu}F_{\alpha\beta\mu\nu}(\mathbf{R}(t)\}, \tag{37}$$

where we have introduced the β state part of the curvature tensor:

$$F_{\alpha\beta\mu\nu} = [(V_\alpha^\dagger \partial_\mu V_\beta)(V_\beta^\dagger \partial_\nu V_\alpha) - (V_\alpha^\dagger \partial_\nu V_\beta)(V_\beta^\dagger \partial_\mu V_\alpha)] \tag{38}$$

and used the fact that on the α orbit we have $H_\alpha = E$.

Equation (37) has a simple interpretation. The first term is the geometric Berry phase while the second term is clearly dynamical and represents the time integral of the classical particle moving through a Hamiltonian phase space endowed with a Berry curvature. Contraction of the Berry curvature with the symplectic matrix yields a scalar, and in the line integral this is, for each semiclassical vector β, weighted by the energy separation of the β manifold and the α-particle orbit: $(H_\beta - E)$.

1. *Structure of the dynamical semiclassical phase*

The structure of the Berry curvature depends, as usual, on the degeneracy structure, in this case of the semiclassical energy manifolds. It is worthwhile exploring this point, and to that end we follow the standard argument and insert the formula for the matrix element of the derivative of an eigenvector to find

$$F_{\alpha\beta\mu\nu} = -\frac{V_\alpha^\dagger(\partial_\mu H)V_\beta V_\beta^\dagger(\partial_\nu H)V_\alpha}{(H_\beta - H_\alpha)^2} + \frac{V_\alpha^\dagger(\partial_\nu H)V_\beta V_\beta^\dagger(\partial_\mu H)V_\alpha}{(H_\beta - H_\alpha)^2}. \tag{39}$$

The structure of $F_{\alpha\beta\mu\nu}$ is thus dominated by degeneracies amongst the classical eigenvalues. The geometric part of the semiclassical phase, of course, depends on the global structure of the Berry curvature $F_{\alpha\mu\nu} = \sum_\beta F_{\alpha\beta\mu\nu}$. This structure is, however, equally important for understanding the dynamical phase (which is local). In particular, if the Berry curvature is a δ function—the case for which the Berry phase is topological, i.e., depends only on the winding number around the pole—then any classical trajectory that does not pass through such a source will have zero for the line integral in Eq. (37). In other words, *if the semiclassical Berry phase is topological then the semiclassical dynamical phase is zero*. A special case of this is the graphene Dirac-Weyl Hamiltonian in the presence of arbitrary $V(\mathbf{r})$ but with no mass term $\sigma_z\phi(\mathbf{r})$. In such a situation, the degeneracy at the Dirac point is preserved, the curvature retains the δ function structure, and hence the semiclassical phase will coincide with the Berry phase, as stated by Carmier and Ullmo [23].

2. *Generalization to the degenerate case*

We wish here to sketch the appropriate generalization to the case of global degeneracies. In this circumstance the semiclassical phase is matrix valued and will in general not commute at different times. Following the usual approach, this requires the $U(1)$-invariant Berry curvature be replaced by the appropriate $U(N)$-covariant curvature $F_{\alpha\mu\nu} = \partial_\mu A_{\alpha\nu} - \partial_\nu A_{\alpha\mu} + i[A_{\alpha\mu}, A_{\alpha\nu}]$. Insertion of the identity operator then yields

$$F_{\alpha\mu\nu} = i\sum_{\alpha\neq\beta} [(V_\alpha^\dagger \partial_\nu V_\beta)(V_\beta^\dagger \partial_\mu V_\alpha) - (V_\alpha^\dagger \partial_\mu V_\beta)(V_\beta^\dagger \partial_\nu V_\alpha)], \tag{40}$$

which is, except for the additional condition of $\alpha \neq \beta$ in the sum, identical to Eq. (35). Note that in this expression the V_α are now $m_\alpha \times n$ matrices, with m_α being the order of the αth degeneracy and n being the dimension of the matrix Hamiltonian.

This similarity between the Berry curvature expressed in the form given by Eqs. (35) and (40) renders the analysis formally similar for the Abelian and non-Abelian cases *at any instant in time*. At any given time, the M_α phase may be decomposed into a part that is a Berry connection and a part that is the curvature of the connection. However, the fact that the time-ordered exponential must be evaluated excludes the possibility of writing the time integral of M_α, i.e., the semiclassical phase, as such a decomposition.

B. Treating the case of orbit degeneracies

If the Hamiltonian has one or more cyclic coordinates, then the stationary phase approximation for these coordinates cannot be applied. Furthermore, if orbits are not isolated, the trace over starting positions is not given by the integral $\oint \frac{dx_\parallel}{\dot{x}_\parallel} = T^p$ as this clearly assumes a single closed orbit (here T^p, as before, denotes the time period of a primitive orbit, i.e., the time to travel once around a closed orbit). We consider here the case where only one coordinate x_n is noncyclic and indicate how this result may be (straightforwardly) generalized. The method presented here differs from that of Carmier and Ullmo [23] in that we derive a solution constructively, beginning at the level of the transport equation, whereas in Ref. [23] the treatment of orbit degeneracies is performed subsequent to a general solution of the transport equation. The two methods are, however, equivalent.

For the case of a single noncyclic coordinate, the transport equation takes on the much simpler form

$$\left(\frac{1}{2}\partial_n\partial_{p_n} + \frac{d}{dt} + iM_\alpha\right)\hat{f}_\alpha = 0 \tag{41}$$

with the solution

$$\hat{f}_\alpha = \sqrt{\frac{\left(\frac{\partial p_n^\alpha}{\partial x_n'}\right)}{\left(\frac{\partial p_n^{\alpha'}}{\partial x_n'}\right)}}\hat{h}_\alpha \tag{42}$$

and this result for f_α gives a new expression for the time-dependent Green's function:

$$G(\mathbf{r},\mathbf{r}',t) \approx \int \frac{dp_1...dp_{n-1}}{i^{1/2}(2\pi\hbar)^{d-1/2}} \sum_{\alpha,\gamma_t} g_{\alpha,\gamma_t}\hat{V}_{\alpha,\gamma_t}(\mathbf{r},\mathbf{r}')$$
$$\times \hat{h}_{\alpha,\gamma_t}(\mathbf{r},\mathbf{r}')\hat{V}^\dagger_{\alpha,\gamma_t}(\mathbf{r},\mathbf{r}')e^{\frac{i}{\hbar}S_{\alpha,\gamma_t}(\mathbf{r},\mathbf{r}',t)-i\frac{\pi}{2}\nu_{\alpha,\gamma_t}}, \tag{43}$$

where

$$g_{\alpha,\gamma_t} = \sqrt{\left|-\frac{\partial(p_{\alpha,\gamma_t},t)}{\partial(x_n',t)}\right|}, \tag{44}$$

while similarly for the energy-dependent Green's function we find

$$G(\mathbf{r},\mathbf{r}',E) \approx \int \frac{dp_1...dp_{n-1}}{i\hbar(2\pi\hbar)^{d-1}} \sum_{\alpha,\gamma_E} g_{\alpha,\gamma_E}$$
$$\times \hat{V}_{\alpha,\gamma_E}(\mathbf{r},\mathbf{r}')\hat{h}_{\alpha,\gamma_E}(\mathbf{r},\mathbf{r}')\hat{V}^\dagger_{\alpha,\gamma_E}(\mathbf{r}',\mathbf{r}')$$
$$\times e^{\frac{i}{\hbar}S_{\alpha,\gamma_E}(\mathbf{r},\mathbf{r}',E)-i\frac{\pi}{2}\nu_{\alpha,\gamma_E}}, \tag{45}$$

where

$$g_{\alpha,\gamma_E} = \sqrt{\left|-\frac{1}{\dot{x}^\alpha_{n\alpha,\gamma_E}\dot{x}^{\alpha'}_{n\alpha,\gamma_E}}\right|}. \tag{46}$$

From the energy-dependent Green's function may then be found the oscillatory part of the density of states:

$$d_{\mathrm{osc}}(E) = 2\int\sum_{\alpha,\gamma_E^\circ} \frac{d^dx dp_{1,\alpha,\gamma_E^\circ}...dp_{n-1,\alpha,\gamma_E^\circ}}{(2\hbar\pi)^d}\frac{1}{\left|\dot{x}_n^{\alpha,\gamma_E^\circ}\right|}$$
$$\times \mathrm{Im}\big[ie^{\frac{i}{\hbar}S_{\alpha,\gamma_E^\circ}-i\frac{\pi}{2}\nu_{\alpha,\gamma_E^\circ}}\mathrm{tr}(\hat{h}_{\alpha,\gamma_E^\circ})\big]. \tag{47}$$

For problems with only one noncyclic coordinate, the 0-length orbit contribution to the density of states has a very similar form:

$$d_0(E) = \int \frac{d^dxd^dp_\alpha}{(2\pi\hbar)^d}\delta(E-H_\alpha)$$
$$= \sum_{\gamma_E^\circ}\int\frac{d^dxd^dp_\alpha}{(2\pi\hbar)^d}\delta\left[\frac{\partial H_\alpha}{\partial p_n}\bigg|_{\gamma_E^\circ}\big(p_n - p_{n\gamma_E^\circ}\big)\right.$$
$$\left.+\frac{\partial H_\alpha}{\partial x_n}\bigg|_{\gamma_E^\circ}\big(x_n - x_{n,\gamma_E^\circ}\big)\right]$$
$$\approx \sum_{\gamma_E^\circ}\int\frac{d^dxdp_{1,\alpha,\gamma_E^\circ}\dots dp_{n-1,\alpha,\gamma_E^\circ}}{(2\pi\hbar)^d}\frac{1}{\left|\dot{x}_{n,\alpha,\gamma_E^\circ}\right|}, \tag{48}$$

where objects with the index γ_E° label different solutions to the Hamilton-Jacobi equations. Consistent with the notion that we are treating very small action orbits, we have expanded the argument of the Dirac δ function about zero position and momentum, deployed a 0-length approximation $(x_n - x_{n,\gamma_E^\circ}) \approx 0$, and subsequently used Hamilton's equation to arrive at the final result.

It is straightforward to generalize the procedure to problems with arbitrary combinations of cyclic and noncyclic coordinates with the only change for more than one noncyclic coordinate is the reappearance of a monodromy matrix in the density of states which is, however, then restricted to the space of the noncyclic coordinates.

C. Density of states for 1D problems: A generalized Bohr-Sommerfeld quantization condition

The modification of the Bohr-Sommerfeld quantization condition for the case of multicomponent WKB as been considered by a number of authors [6–10]. In the general formalism we espouse here, a Bohr-Sommerfeld condition follows straightforwardly, providing that the following assumptions hold: (i) there is no global degeneracy, (ii) the action, the semiclassical phase, and the Maslov index are all independent of initial positions, and (iii) there are no position-dependent prefactors of the momentum terms. Under these conditions $d_0(E)$ and $d_{\mathrm{osc}}(E)$ may be combined and the Dirac comb identity used to yield a compact expression for density of states:

$$d(E) = d_0(E) + d_{\mathrm{osc}}(E)$$
$$= \int\sum_{\alpha,\gamma_{E,p}^\circ,n}\frac{d^dxdp_{1,\alpha,\gamma_{E,p}^\circ}\dots dp_{n-1,\alpha,\gamma_{E,p}^\circ}}{(2\hbar\pi)^d}\frac{1}{\left|\dot{x}_n^{\alpha,\gamma_{E,p}^\circ}\right|}$$
$$\times\delta\left(\frac{S_{\alpha,\gamma_{E,p}^\circ}}{2\pi\hbar}-\frac{\nu_{\alpha,\gamma_{E,p}^\circ}}{4}+\frac{1}{2\pi}\int_0^{T_{\alpha,\gamma_{E,p}^\circ}}dtM_\alpha - n\right), \tag{49}$$

where $\gamma_{E,p}^\circ$ denotes once more a primitive orbit. From the δ function one can then read off a generalization of the Bohr-Sommerfeld quantization condition:

$$\frac{S_{\alpha,\gamma_{E,p}^\circ}}{2\pi\hbar}-\frac{\nu_{\alpha,\gamma_{E,p}^\circ}}{4}+\frac{1}{2\pi}\int_0^{T_{\alpha,\gamma_{E,p}^\circ}}dtM_\alpha - n = 0. \tag{50}$$

D. Summary of semiclassical steps towards the density of states

We briefly present a summary of the steps required to obtain the oscillatory density of states for a generic matrix Hamiltonian $\hat{H}(-i\hbar\partial_i,x_i)$:

1. Reverse quantization

In the Hamiltonian $\hat{H}(-i\hbar\partial_i,x_i)$ replace $-i\hbar\partial_i \to p_i = \partial_i S$. One thus finds the matrix $H(p_i,x_i)$.

2. Introducing a set of classical particle types

Determine the eigenvalues H_α of $H(p_i,x_i)$ and corresponding normalized eigenvectors $\hat{V}_\alpha$ for $E\hat{V} = \hat{H}(p_i,x_i)\hat{V}$. In the case of degenerate eigenvalues H_α, orthonormalize the corresponding eigenvectors and write them next to each other as columns giving the "full eigenvector" $\hat{V}_\alpha$ (an $m_\alpha \times n$ matrix with m_α the degeneracy number of the αth set of distinct eigenvalues).

3. Solving the classical problems

The eigenvalues H_α correspond to Hamilton-Jacobi equations $E = H_\alpha$, which must be solved for the actions $S_{\alpha,\gamma_E^\circ}$ of all periodic orbits γ_E° at energy E.

4. Determining the Maslov indices

Calculate the Maslov index $\nu_{\alpha,\gamma_E^\circ}$ for each orbit, which is given by the sum of all sign changes of (i) $\dot{r}^{\parallel}_{\alpha,\gamma_E^\circ}$ (the velocity along the orbit) and (ii) $\det(\mathbb{1}_{2(d-1)} - \mathbb{J}_{\alpha,\gamma_E^\circ})$ [see Eq. (26) for the definition of $\mathbb{J}_{\alpha,\gamma_E^\circ}$]. In the case of a one-dimensional problem, the Maslov index is just the number of classical wall reflections (i.e., sign changes of $\frac{\partial p}{\partial x}$) along the orbit in phase space.

5. Evaluation of $\hat{\Lambda}$

For the case in which there are coordinate function prefactors to derivatives in the Hamilton operator, one also has to calculate $\hat{\Lambda}$ using Eq. (15).

6. Calculating the semiclassical phase

Express the $V_{\alpha,\gamma_E^\circ}$ in terms of x_i and use Eq. (29) to calculate M_α.

7. The density of states

The expressions resulting from the previous steps must then be entered into Eq. (26) or, in the case of nonisolated orbits and cyclic coordinates, into Eq. (47) and the integrals over the cyclic coordinates performed.

The procedure for obtaining the semiclassical Green's functions is almost the same; however, it includes nonclosed orbits and, as is well known (see, for example, Ref. [42]), classification of all possible such orbits is a difficult problem, and this procedure is rarely used to explicitly evaluate the Green's function.

The above steps present a systematic recipe for calculating the semiclassical density of states of an arbitrary matrix-valued Hamiltonian. In the next two sections, we will apply this procedure first to a number of systems for which the exact quantum mechanical result is known (Sec. III), as well as subsequently (Sec. IV) to a problem, the one-dimension strain moiré in bilayer graphene, for which the quantum result may only be obtained numerically (the semiclassical result, however, remains of simple analytical form).

III. SEMICLASSICS FOR EXACTLY SOLVABLE SYSTEMS

As a first test of the semiclassical procedure outlined in the previous sections, we consider a number of cases for which the exact analytical solution is known.

A. Single-layer graphene

We first consider a single layer of graphene in a uniform out-of-plane magnetic field. The Hamiltonian is thus simply the Dirac-Weyl operator with minimal substitution:

$$\hat{H}_g = v_F \hat{\boldsymbol{\Pi}}\boldsymbol{\sigma}; \quad \Pi_1 = \hbar k_1 + eBx_2; \quad \Pi_2 = -i\hbar\partial_2, \tag{51}$$

and where we have employed the Landau gauge so that k_1 is a good quantum number of the problem. This system has been treated by Carmier and Ullmo [23], and we thus omit details of the derivation. The final result, which agrees with that given in Ref. [23], is given by

$$\begin{aligned} d(E) &= \sum_{n=-\infty}^{\infty} \frac{A|E|}{\hbar^2 v_F^2}\delta\left(\frac{E^2}{2v_F^2 eB\hbar} - n\right) \\ &= \frac{eBA}{2\pi\hbar}\sum_{n=-\infty}^{\infty}\delta(E - E_n). \end{aligned} \tag{52}$$

B. Four-band model of bilayer graphene

A much more difficult system to treat in any method that employs a matching procedure is the full four-band model of AB stacked bilayer graphene (in Ref. [23] only the two band down-folded version of the full Hamiltonian was treated). We take the simplest model of this material in which the interlayer coupling matrix T is independent of momentum (although lifting this condition would not significantly complicate the analysis),

$$\hat{H}_{\text{ABbi}} = \begin{pmatrix} \hat{H}_g & T \\ T^\dagger & \hat{H}_g \end{pmatrix}; \quad T = \begin{pmatrix} 0 & \tau \\ 0 & 0 \end{pmatrix}, \tag{53}$$

where τ describes the interlayer hopping. With the method outlined in the previous section, this system yields straightforwardly to a semiclassical analysis as we now show. We first send $-i\hbar\partial_i \to p_i = \partial_i S$ and diagonalize the resulting Hamiltonian to find the eigenvalues

$$E = s_1\left(\frac{\tau}{2}\right) + s_2\left[\left(\frac{\tau}{2}\right)^2 + (v_F\Pi)^2\right]^{(1/2)}, \tag{54}$$

where $\Pi^2 = [(\hbar k_1 + eBx_2)^2 + p_2^2]$ and $s_{1,2} = \pm 1$ label the four bands; the low-energy chiral bands have $s_1 s_2 = -1$ and the high-energy bonding and antibonding bands $s_1 s_2 = +1$. The corresponding eigenvectors are

$$V_{s_1 s_2} = \begin{pmatrix} E \\ v_F \Pi s_2 e^{i\theta} \\ s_1 s_2 E \\ s_1 v_F \Pi e^{-i\theta} \end{pmatrix}, \tag{55}$$

where $\theta = \tan^{-1} \Pi_1/p_2$ and where $\Pi_1 = \hbar k_1 + eBx_2$. These are, of course, are formally identical to the standard eigenvalues and eigenvectors of the Bernal bilayer. Equation (54) may be straightforwardly solved for p_2 and then the action found from $S = \int p_2 dx_2$, giving

$$S = \frac{\pi E(E - s_1\tau)}{eBv_F^2}. \tag{56}$$

From the eigenvectors, the semiclassical M_α phase is immediately found to be zero (the Berry phase is also zero in this system). Note this contrasts with the case of single-layer graphene where the Berry phase is π, and the semiclassical phase equals the Berry phase; i.e., the dynamical phase is zero. This is a consequence of the δ-function structure of the Berry curvature for single-layer graphene. The Maslov index is $\nu_{\alpha\gamma_E^\circ} = 2$ since there are only two turning points independent of the initial position of the classical orbits, we can deploy Eq. (50) to immediately find the semiclassical spectrum

$$\frac{\epsilon(\epsilon - s_1)}{C} = n - \frac{1}{2}, \tag{57}$$

where $C = \frac{2\hbar eB}{\tau^2}$ and $\epsilon = \frac{E}{\tau}$. The exact quantum solution is given as

$$\epsilon^2 = \left[C\left(n + \frac{1}{2}\right) + \frac{1}{2}\right] \pm \sqrt{\left[C\left(n + \frac{1}{2}\right) + \frac{1}{2}\right]^2 - C^2 n(n+1)}. \tag{58}$$

For large n, the limit in which the semiclassical approximation must hold, we find

$$\epsilon = s_1\sqrt{Cn} + \sigma_2\frac{1}{2} + \sigma_1\frac{1+2C}{8\sqrt{Cn}} + \mathcal{O}(n^{-\frac{3}{2}}) \tag{59}$$

for our approximation, while from the exact result we find

$$\epsilon = s_1\sqrt{Cn} + \sigma_2\frac{1}{2} + \sigma_1\frac{1+2C}{8\sqrt{Cn}} + \sigma_2\frac{C}{16n} + \mathcal{O}(n^{-\frac{3}{2}}). \tag{60}$$

Thus, the semiclassical result agrees up to $\mathcal{O}(n^{-\frac{1}{2}})$ with the exact result, and the agreement for smaller magnetic fields is better as can be seen by the fact that the higher order terms depend on C, which is essentially the magnetic field.

For both of these example problems, (i) the Hamilton-Jacobi equations were nondegenerate and (ii) the dynamical part of the semiclassical phase vanished (and thus the semiclassical phase was identical to the Berry phase). We now turn to a problem which is both nondegenerate and, as we shall see, one in which the dynamical phase is nonzero.

C. Silicene

Silicene is two-dimensional allotrope of silicon with a hexagonal honeycomb structure similar to that of graphene. Spin-orbit coupling is more important in this material than in graphene (where it can generally be neglected), and therefore in the treatment that follows the spin-orbit coupling term is included. The Hamiltonian for this system is given as [46]

$$\begin{aligned} H = {} & v_2(\sigma_1 \otimes \mathbb{1}_2 \hat{p}_1 + \sigma_2^* \otimes \mathbb{1}_2 \hat{p}_2) \\ & - v_1\left(\sigma_3 \otimes \sigma_1 \hat{p}_2 + \sigma_3 \otimes \sigma_2 \hat{p}_1 + \sigma_3 \otimes \sigma_3 m\frac{v^2}{v_1}\right), \end{aligned} \tag{61}$$

where $\otimes$ is the tensor product for matrices and we use the basis $\{|A\rangle, |B\rangle\} \otimes \{|\uparrow\rangle, |\downarrow\rangle\}$ (see Ref. [46] for details of this model Hamiltonian). The term proportional to the Fermi velocity, v_1, is just the graphene Hamiltonian with a mass term m, while the term proportional to v_2 describes spin-orbit coupling.

We will consider silicene in an uniform out-of-plane magnetic field and therefore introduce into Eq. (61) the minimal substitution $\hat{p}_1 \to \hat{\Pi}_1 = \hat{p}_1 + eBx_2$. Replacing momentum operators by momentum functions $\hat{p}_i \to p_i$ in the resulting Hamiltonian yields the matrix $H(p_i, x_i)$, diagonalization of which results in two pairs of twice-degenerate eigenvalues and thus twice-degenerate Hamilton-Jacobi equations. These are given as

$$E = \pm\sqrt{m^2v^4 + v^2\left(p_1^2 + p_2^2\right)} =: \pm h \tag{62}$$

and evidently describe a relativistic particle with a speed of light $v = \sqrt{v_1^2 + v_2^2}$ and mass energy mv^2. The corresponding full eigenvectors are

$$-V_+ = \begin{pmatrix} 0 & -\frac{v(ip_2+p_1)}{\sqrt{2}\sqrt{h(h-mv^2)}} \\ \frac{v_2(ip_2+p_1)}{\sqrt{2}\sqrt{h(h+mv^2)}} & \frac{i(mv^2-h)v_1}{\sqrt{2}\sqrt{h(h-mv^2)}v} \\ \frac{v_1(p_2-ip_1)}{\sqrt{2}\sqrt{h(h+mv^2)}} & \frac{\left(mv^2-h\right)v_2}{\sqrt{2}\sqrt{h(h-mv^2)}v} \\ \frac{\sqrt{h(h+mv^2)}}{\sqrt{2}h} & 0 \end{pmatrix} \tag{63}$$

and

$$V_- = \begin{pmatrix} 0 & -\frac{v(ip_2+p_1)}{\sqrt{2}\sqrt{h(h+mv^2)}} \\ \frac{v_2(ip_2+p_1)}{\sqrt{2}\sqrt{h(h-mv^2)}} & \frac{i(h+mv^2)v_1}{\sqrt{2}\sqrt{h(h+mv^2)}v} \\ \frac{v_1(p_2-ip_1)}{\sqrt{2}\sqrt{h(h-mv^2)}} & \frac{\left(h+mv^2\right)v_2}{\sqrt{2}\sqrt{h(h+mv^2)}v} \\ \frac{\sqrt{h(h-mv^2)}}{\sqrt{2}h} & 0 \end{pmatrix}. \tag{64}$$

The action is easily found from these Hamilton-Jacobi equations, Eq. (62), to be $S_{\alpha,r} = r\pi\frac{E^2-m^2v^4}{2eBv^2}$, and the Maslov index to be $2r$ with r the number of circuits of one primitive orbit. From the full eigenvectors we find the (matrix-valued) semiclassical phase to be

$$\begin{aligned} \int_0^T dt M_\pm &= -i\pi\frac{\sqrt{E^2 - m^2v^4}}{E}\mathbb{1}_2 \\ &= -i\pi\mathbb{1}_2 - \frac{1}{2}\frac{m^2v^4}{E^2}\mathbb{1}_2 + \mathcal{O}\left(\frac{m^4v^8}{E^4}\right). \end{aligned} \tag{65}$$

The expression for $M_\pm$ itself is diagonal (yet this is generally not the case; see, for example Ref. [17]). On the other hand, the Berry phase can also be calculated directly from the full eigenvectors and is found to be

$$\int_0^T dt M_\pm^1 = -i\pi\mathbb{1}_2 - i\frac{mv^2}{E}\sigma_3, \tag{66}$$

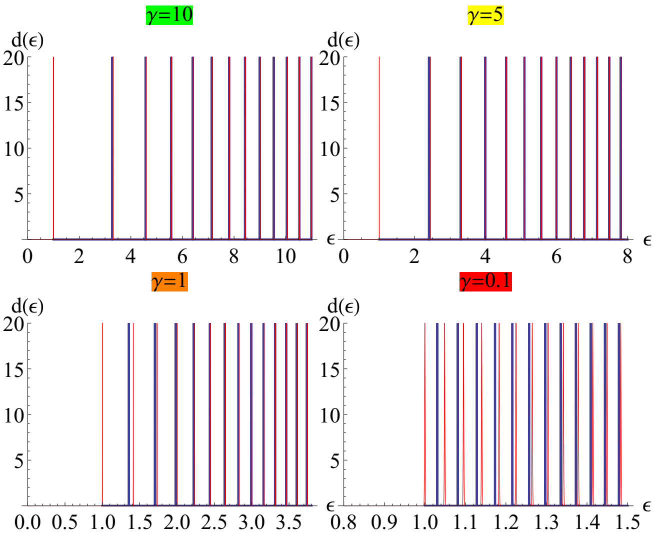

FIG. 1. Plot of the exact (red) and semiclassical (blue) silicene density of states for different values of $\gamma = \frac{2eBv^2}{m^2v^4}$.

which clearly does not coincide with the full semiclassical phase, Eq. (65). It is interesting to note that both phases coincide in the limit $E \gg mv^2$, where they limit to the energy-independent constant $i\pi\mathbb{1}_2$, but the next order of the semiclassical phase is quadratic in $1/E$ while it is linear for the Berry phase.

As both the semiclassical phase and the Maslov index do *not* depend on initial positions, we may use directly the generalized Bohr-Sommerfeld quantization condition, Eq. (50). To this end, we require the maximum initial momentum in the cyclic direction and this provides the bounds for the cyclic momentum integral, which can straightforwardly be found from the Hamilton-Jacobi equations as $\Pi = \frac{\sqrt{E^2-m^2v^4}}{v}$. We hence encounter the integral $\int \frac{dp_1'}{|\dot{x}_2|} = \int_0^{2\pi} \frac{\Pi d\theta}{v} = \frac{2\Pi\pi}{v}$ and hence the density of states is given by

$$d(E) = \sum_{n=-\infty} \frac{2A\sqrt{E^2-m^2v^4}}{(\hbar v)^2} \times \delta\left(\frac{E^2-m^2v^4}{2eB\hbar v^2} - \frac{\sqrt{E^2-m^2v^4}}{2E} - \frac{1}{2} - n\right). \quad (67)$$

The exact energy levels are given as $\frac{E}{mv^2} = \epsilon = \pm\sqrt{1+n\gamma}$, where $\gamma = \frac{2eBv^2}{m^2v^4}$, and we thus see that in the $E \gg mv^2$ limit of the semiclassical phase we obtain the exact result. This implies that, as the semiclassical phase is $\mathcal{O}(1/E^2)$ and the Berry phase $\mathcal{O}(1/E)$, the extra dynamical term in the semiclassical phase is important. In Fig. 1, we present a graphical comparison of the exact and semiclassical energy levels and, as may be seen, while the disagreement is pronounced at low energies, for higher energies the agreement is, as expected, very good.

IV. THE STRAIN MOIRÉ

We now consider the semiclassical analysis of a complex graphene system that is an analog of the well-studied graphene twist bilayer, the one-dimensional strain moiré. As may be seen in Fig. 2, this consists of a uniform strain applied to (without loss of generality) layer 1 of an initially AB stacked bilayer that leads to a moiré lattice in which (as in the case of the twist bilayer) all possible stacking types occur over one moiré period. We choose to apply the strain in the armchair direction (x_2 in the coordinate system displayed in Fig. 2) as this makes the semiclassical analysis somewhat more tractable. The deformation field of the problem is therefore, using the coordinate system indicated in Fig. 2, given by $\Delta\mathbf{u}(x_2) = [0,a(x_2)]$, and it is convenient to express this as $a(x_2) = \sqrt{3}\frac{\gamma(x_2)}{2\pi} + \frac{1}{\sqrt{3}}$ with $\gamma(x_2)$ being some function encoding the particular strain and the constant shift term introduced for a more symmetrical Hamiltonian. With these definitions, the interlayer potential $S(\gamma)$ can be obtained via the general theory outlined in Ref. [47] with the result

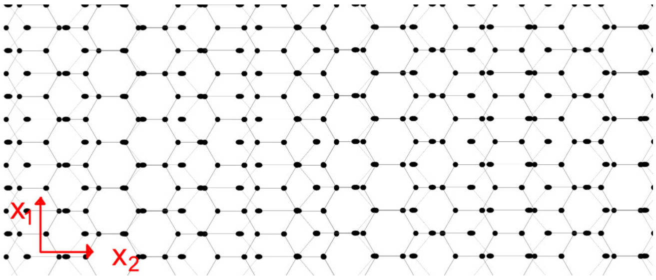

FIG. 2. The graphene strain moiré: Uniform strain is applied in the armchair direction to one layer of an initially AB stacked bilayer.

$$S(\gamma) = t\begin{pmatrix} 1-\cos\gamma-\sqrt{3}\sin\gamma & 1+2\cos\gamma \\ 1+2\cos\gamma & 1-\cos\gamma+\sqrt{3}\sin\gamma \end{pmatrix}, \quad (68)$$

where $t = \tau/3$ with $\tau = 0.4$ eV being the interlayer hopping. The Hamiltonian of the strain moiré system is then given by

$$H = \begin{pmatrix} \boldsymbol{\sigma}\mathbf{p} & S(\gamma) \\ S(\gamma)^\dagger & \boldsymbol{\sigma}^*\mathbf{p} \end{pmatrix}. \quad (69)$$

Note that this interlayer field is rather similar to that deployed for the one-dimensional moiré treated in Ref. [36]; however, in that work the moiré was created by shear and not by strain. The system we consider here was, however, recently treated in Ref. [48] and we will comment on the agreement between our semiclassical theory and this work at the end of this section. Uniform strain requires $\gamma(x_2) = 2\pi\frac{x_2}{L}$, with L the moiré period as may be deduced from Eq. (68). In particular, we have AA stacking at $2\pi n$, AB stacking at $2\pi n + 2\pi/3$, and AC stacking at $2\pi n + 4\pi/3$, as may readily be seen by substitution of these γ values into Eq. (68). Solving the classical $\mathcal{O}(\hbar^0)$ problem, we find four nondegenerate Hamilton-Jacobi systems. Evidently p_1 is a good quantum number of the effectively one-dimensional problem, and for simplicity we will consider here the case $p_1 = 0$; this is not a singular limit and as such the small p_1 behavior is very similar to $p_1 = 0$. For larger p_1, the system develops a much richer and interesting structure, which we will not investigate here. The four distinct Hamilton-Jacobi equations have four distinct

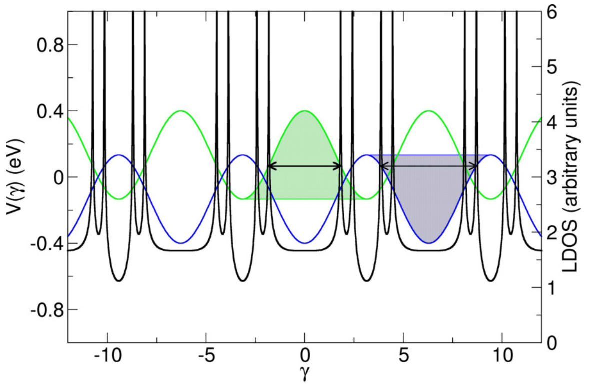

FIG. 3. Structure of the classical orbits for for a strain moiré ($L = 1000\,\mathrm{nm}$). The effective potentials of particle types 1 and 2 are shown as the blue and green lines, respectively, with the shaded areas illustrating the classically allowed regions; note that this is inverted for particle type 2 due to the negative effective mass of that particle type; see Eq. (71). For an energy of $E = 0.067\,\mathrm{eV}$, the two orbits of the two particle types are indicated, along with the corresponding local density of states. This latter quantity displays, as expected, pronounced peaks at the turning points of the classical particle. The AA spots of the moiré correspond to $\gamma = 2\pi n$ with $\gamma = 2\pi x_2/L$.

momenta, of which two differ only by a minus sign:

$$p_2^{1,2,\pm} = \pm\sqrt{2m^*_{1,2}(E)[E + V_{1,2}(\gamma)]}, \tag{70}$$

where the index ± indicates the sign in front of the square root. For simplicity of discussion, we will now adopt the habit of referring to the solution with indexes 1 and 2 as particles 1 and 2. In Eq. (70), we have expressed the momenta in terms of an effective mass m^* given by

$$m^*_{1,2}(E) = \frac{E \pm 3t}{2}, \tag{71}$$

which is energy dependent, and an effective potential $V_{1,2}(\gamma)$ that takes the form

$$V_{1,2} = \pm t(1 + 2\cos\gamma). \tag{72}$$

The cosine form of this potential reveals immediately that we have a quantum well structure to the problem with the maxima (particle type 1) or minima (particle type 2) centered at the AA spots $\gamma = 2\pi n$. For particle type 1, the effective mass is negative at all E where $V(\gamma)$ is defined, the usual regions of classically allowed and forbidden motion are inverted, and thus a maxima of the effective potential at the AA spot indicates bound orbits centered on this region of the moiré. Particle type 2 with a minimum of the potential well on the AA spot and a positive mass well evidently also describes orbits centered at the AA spot. This is illustrated in Fig. 3 in which the shaded areas represent the regions of allowed particle motion and one can see that the situation is symmetric if we send particle type 1 to 2 and $E \to -E$ provided the sign of the mass changes as well.

To examine this situation more closely, we determine the turning points of the orbits which for particle type 1 are given by

$$x_i^1 = 2\pi n - \cos^{-1}\left(\frac{E - t}{2t}\right), \tag{73}$$

$$x_f^1 = 2\pi n + \cos^{-1}\left(\frac{E - t}{2t}\right), \tag{74}$$

and for particle type 2 by

$$x_i^2 = 2\pi n - \cos^{-1}\left(\frac{-E - t}{2t}\right), \tag{75}$$

$$x_f^2 = 2\pi n + \cos^{-1}\left(\frac{-E - t}{2t}\right). \tag{76}$$

The orbit length for particle 2 is given by $l_1 = 2\cos^{-1}(\frac{E-t}{2t})$ and (as may also be seen from Fig. 3) decreases with increasing E until we find a zero-length orbit at the band edge $E = 3t = \tau$, after which the particle trajectory abruptly jumps from a zero-length orbit to nonlocalized behavior. In contrast, there are no bound states of this particle type at the other band edge of $E = -3t = -\tau$ as at $E = -t$ the bound orbits merge together, and the behavior for energies lower than this is again nonlocalized. For particle type 1, the situation is the same but with $E \to -E$. Interestingly, and contrary to what one might expect given the results of the previous section, the semiclassical approximation for the strain moiré is therefore *better for lower energies than for large energies*, in particular close to band edges where the approximation is guaranteed to fail as the orbit length approaches zero. On the other hand, one should stress that for slowly varying structural perturbations—such as considered here—the semiclassical approximation is expected to be good. To calculate the semiclassical spectrum via the Gutzwiller formula, we require the semiclassical phase, the actions S, and the orbit times T. We now proceed to calculate each of these in turn.

A. The semiclassical phase

The integral of the M phase $I_\alpha = \oint dt M_\alpha$ may be conveniently found by the change of variables

$$\begin{aligned}\oint dt M_\alpha(t) &= \oint dt \hat{V}_\alpha^\dagger \partial_{p_\mu} H_{cl} \frac{d}{dx_2} \hat{V}_\alpha \\ &= \oint dt \frac{d\gamma}{dx} \hat{V}_\alpha^\dagger \partial_{p_\mu} H_{cl} \frac{d}{d\gamma} \hat{V}_\alpha \\ &=: \oint \frac{d\gamma}{\dot{x}(\gamma)} \tilde{M}_\alpha(\gamma)\end{aligned} \tag{77}$$

and is found to be

$$I_1 = \begin{cases} -2\pi; & -t < E < 0 \\ -\pi; & E = 0 \\ 0; & 3t > E > 0 \end{cases}, \tag{78}$$

where we also find, as we must, that $I_2 = I_1(E \to -E)$. In fact, only the result for $E = 0$ could be obtained fully analytically; for $E > 0$ and $E < 0$ the integral was taken numerically with the values -2π and 0 obtained to 10^{-8} accuracy.

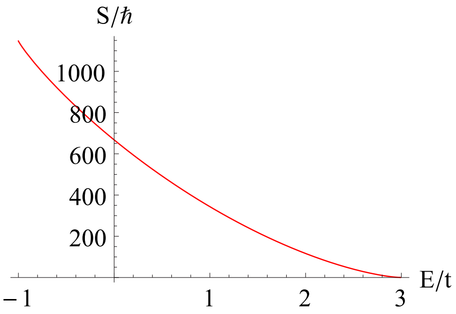

FIG. 4. Plot of the action for particle type 2 in a strain moiré with $L = 1000$ nm, $v_F = 0.003c$, and $\tau = 0.4$ eV.

B. The action S

The actions may be obtained analytically from the Hamilton-Jacobi equations with the result that

$$S_1 = \frac{4L(3t-E)\mathcal{E}\left[\frac{1}{2}\sec^{-1}\left(\frac{2t}{E-t}\right),\frac{4t}{3t-E}\right]}{\pi v_F} \tag{79}$$

for particle type 1, where $\mathcal{E}(a,b)$ is the elliptic integral of the second kind. For particle type 2, we simply have $S_2 = S_1(E \to -E)$. The action for particle type 2 is shown in Fig. 4, and evidently is larger for smaller energies and large compared to $\hbar$, thus justifying the semiclassical approximation at low energies.

C. Orbit times

The time for an orbit T_α can be found as $T_\alpha = \int dt = 2\int_{x_i^\alpha}^{x_f^\alpha} dx_2 \frac{1}{\dot{x}_2}$, where

$$\dot{x}_2^{1,2} = \pm\frac{v_F\sqrt{(E-3t)(E-2t\cos\gamma-t)}}{E-t\cos\gamma-2t}, \tag{80}$$

$$\dot{x}_2^{3,4} = \dot{x}_2^{1,2}(E \to -E), \tag{81}$$

which follows from the Hamilton's equations and which we calculated using the Hellman-Feynman theorem $\partial_{p_2^\alpha} H_\alpha = \partial_{p_2}\hat{V}_\alpha^\dagger H(p_2,x_2)\hat{V}_\alpha = \hat{V}_\alpha^\dagger \partial_{p_2} H(p_2,x_2)\hat{V}_\alpha$. We thus arrive at the following expression for the period T_α:

$$T_1 = \frac{2L}{\pi v_F}\left\{\mathcal{F}\left[\frac{1}{2}\sec^{-1}\left(\frac{2t}{E-t}\right),\frac{4t}{3t-E}\right] + \mathcal{E}\left[\frac{1}{2}\sec^{-1}\left(\frac{2t}{E-t}\right),\frac{4t}{3t-E}\right]\right\}, \tag{82}$$

$$T_2 = T_1(E \to -E), \tag{83}$$

where $\mathcal{F}(a,b)$ is the elliptic integral of the first kind and $\mathcal{E}(a,b)$ is the elliptic integral of the second kind.

We now have all the ingredients required to obtain the semiclassical spectrum via the Gutzwiller trace formula. As all of these quantities evidently do not depend on the initial position of the orbit, we may use the generalized Bohr-Sommerfeld quantization condition, Eq. (50). We note that in a sample of length L_L the orbits are, evidently, L_L/L-times degenerate and the resulting density of states is then

$$d(E) = \frac{L_L}{L}\sum_{n=-\infty}^{\infty}\left[\frac{T_1}{\hbar\pi}\delta\left(\frac{S_1}{2\pi\hbar}+\frac{I_1^M}{2\pi}-n-\frac{1}{2}\right) + \frac{T_2}{\hbar\pi}\delta\left(\frac{S_2}{2\pi\hbar}+\frac{I_2^M}{2\pi}-n-\frac{1}{2}\right)\right]. \tag{84}$$

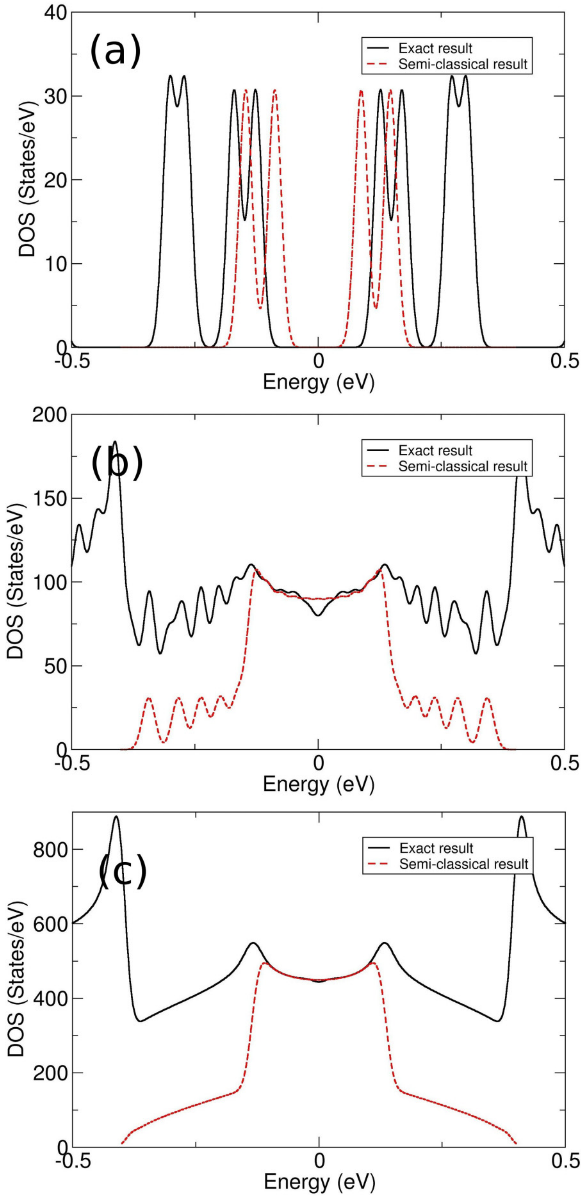

FIG. 5. Plot of the Gaussian smoothed density of states for both the semiclassical approximation (red), Eq. (84), compared to the exact quantum result obtained by diagonalization of Eq. (69) (black). Shown are strain moiré systems with moiré lengths of $L = 10$ nm (a), $L = 100$ nm (b), and $L = 500$ nm (c) showing the increasingly good agreement at low energies between the exact result and semiclassical approximation. Note that by construction the semiclassical approximation only treats bounds orbits, and hence it is only near the Dirac point where bound orbits exist in the strain moiré (but at which the DOS is zero for pristine graphene) that the agreement between the semiclassical and exact solution is very good.

In Fig. 5 we plot this semiclassical density of states against the exact result, obtained simply by solving the quantum problem of Eq. (69) in a basis of single-layer graphene states, for three moiré lengths, $L = 10$, $L = 100$, and $L = 500$ nm. As the moiré length increases, an increasing number of bound states are trapped in the AA centered quantum wells. Interestingly, even for a rather small moiré length of $L = 10$ nm, the four bound states that are trapped in the well are reasonably well described in the semiclassical approximation. As the moiré length increases, the agreement between the semiclassical and exact results becomes increasingly good, with at $L = 500$ nm the low-energy agreement between the two results almost perfect.

We may also calculate the local density of states (LDOS), obtained simply by leaving out the position trace $\int dx_2 \frac{1}{\dot{x}_2}$ in the general formula Eq. (47):

$$d_L(E,x_2) = \frac{L_L}{L} \sum_{n=-\infty}^{\infty} \left[\frac{1}{\hbar\pi\dot{x}_1} \delta\left(\frac{S_1}{2\pi\hbar} + \frac{I_1^M}{2\pi} - n - \frac{1}{2} \right) + \frac{1}{\hbar\pi\dot{x}_2} \delta\left(\frac{S_2}{2\pi\hbar} + \frac{I_2^M}{2\pi} - n - \frac{1}{2} \right) \right]. \tag{85}$$

The LDOS at an energy of $E = 0.067$ eV is shown in Fig. 3 along with the classically allowed orbits indicated by the arrowed lines. Evidently the LDOS shows a pronounced intensity peak at the turning points of the classical orbit, exactly as one would expect. This can also be seen in a density plot of the LDOS as a function of energy and γ, shown in Fig. 6, where we have smoothed the result via a Gaussian convolution for ease of plotting (each eigenvalue is weighted by a Gaussian function with half width 13 meV). The bright high-intensity regions of LDOS follow the turning point structure of the classical orbits and result in regions of high LDOS surrounding the AA spots of the strain moiré. This trapping in the AA regions of the lattice for the case of a strain moiré has recently been described in Ref. [48]. The strain moiré thus represents a one-dimensional analogy of the much more complex twist bilayer system [29], for which trapping in the AA regions is also observed.

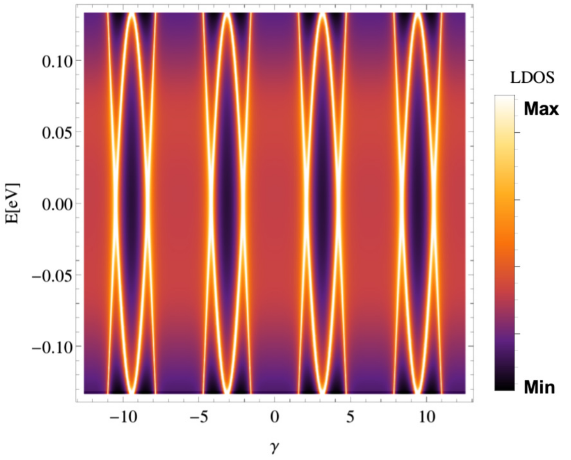

FIG. 6. Plot of the smoothed local density of states for a strain moiré with moiré length $L = 1000$ nm, plotted in the energy position plane. The AA stacked regions of the moiré are at $\gamma = 2\pi n/3$ with n integer, and thus close to $E = 0$ we see clear localization on the AA regions of the lattice. As described in the text, this can be understood as trapping by a semiclassical moiré potential. The high-intensity regions in the LDOS mark the turning points of the classical orbits described by Eqs. (73)–(76).

V. CONCLUSION

For a general $n \times n$ matrix Hamiltonian $H(\hat{\mathbf{p}},\hat{\mathbf{q}})$, we have presented a transparent and physically motivated semiclassical theory and demonstrated its tractability even for realistically complex systems such as the strain moiré in bilayer graphene. We find that the classical dynamics is governed by n Hamilton-Jacobi equations, corresponding to $m \leqslant n$ semiclassical particle types, in a Hamiltonian phase space endowed with a Berry curvature encoding anholonomy in the transport of the eigenvectors of $H(\mathbf{p},\mathbf{q})$ around the classical orbits. While for some systems the semiclassical particle types have an intuitive interpretation, e.g., in the case of the Dirac equation these correspond to electrons and positrons [17], in a more general solid state context these simply represent the emergence of the internal semiclassical structure of the underlying quasiparticles. In particular, the number of semiclassical particle types may be less than n, as was the case for the strain moiré treated in Sec. IV. For each particle type α, we find at $\mathcal{O}(\hbar^1)$ a *transport equation* for the wave-function amplitude, which differs from a similar equation found in the case of a scalar Hamiltonian only by the presence of (i) the semiclassical phase M_α described above and (ii) a real-valued weighting function Λ_α that arises if the Hamiltonian contains momentum operators with position-dependent prefactors (this will arise, for example, in the case of a minimal coupling $[\mathbf{p} + \mathbf{A}(\mathbf{q})]^2$ term).

For the case of nondegenerate Hamilton-Jacobi (HJ) equations, we have shown that M_α can be understood in terms of a $U(1)$ Berry curvature that underpins both the geometric and dynamical phases that M_α can be decomposed into. The latter phase represents, via an integral along the particle orbit of a contraction between the curvature and the symplectic matrix, a dynamical memory of the particle moving through the Berry curvature. In the case of global degeneracies among the HJ systems, M_α becomes matrix valued and the $U(1)$ gauge-invariant Berry curvature goes over to the $U(N)$ gauge-covariant Berry curvature and, although the theory at any instant of time remains formally very similar to the nondegenerate case, noncommutation at different times then precludes the interpretation in terms geometrical and dynamical manifestations of an underlying Berry curvature.

This scheme leads to expressions for the semiclassical Green's functions and the semiclassical density of states, and we have provided such expressions for both the degenerate and nondegenerate cases, as well as for further more specialized situations such as the presence of cyclic coordinates. In particular, for effectively one degree of freedom systems ($n - 1$ cyclic coordinates) we have presented a generalization of the Bohr-Sommerfeld quantization rule for closed orbits.

We have applied this formalism to a number of low-dimensional systems: graphene, Bernal stacked bilayer graphene, silicene, and a one-dimension strain moiré in bilayer graphene. In the latter case we find almost perfect agreement between the exact and semiclassical density of states arising from localized states that the moiré induces near the Dirac point, while for the former cases good agreement is observed between the exact and semiclassical Landau spectra at high energies. Using the formalism here, even the strain moiré yielded rather easily to a semiclassical treatment which, we stress, would be almost impossibly complex to treat with the WKB method, or indeed any approach utilizing a matching condition between wave functions or Green's functions [23].

The semiclassical treatment of the strain moiré reveals the existence of two particle types (that dominate the negative- and positive-energy regions) that for energies near the Dirac point are trapped in a semiclassical potential well centered on the AA stacked regions of the moiré lattice. It should be stressed that such physics is in an essential way semiclassical: At the quantum level a potential well in graphene will not form bound states due to the Klein tunneling effect. The existence of such moiré potential wells has been discussed on the basis of numerical tight-binding calculations in which localization seen on the AA regions of the graphene twist bilayer [36,49,50], a two-dimensional analog of the one-dimensional system considered in this work, but never rigorously shown to exist. Our work shows that this moiré potential well concept is in fact most naturally a semiclassical concept. This illustrates the conceptual usefulness of the semiclassical approach in providing insight into the physics of these complex systems.

As much of the structural complexity of low-dimensional systems is due to deformations that are spatially slow on the scale of the lattice constant, for example, partial dislocation networks in Bernal stacked bilayer graphene [30–32], the formalism presented in this work may provide not only a numerically tractable scheme for such complex systems, but also one which may yield transparent access to the underlying physics of this new class of materials. In addition, the results of this paper may facilitate a treatment of a semiclassical transport in systems with internal degrees of freedom where, in analogy to the scalar case [51], one should be able to find semiclassical expressions for the Kubo conductivity formula.

ACKNOWLEDGMENT

This work was supported by the Collaborative Research Center SFB 953 of the Deutsche Forschungsgemeinschaft (DFG).

---

[1] G. Wentzel, Eine verallgemeinerung der quantenbedingungen für die zwecke der wellenmechanik, Z. Phys. **38**, 518 (1926).

[2] H. A. Kramers, Wellenmechanik und halbzählige quantisierung, Z. Phys. **39**, 828 (1926).

[3] L. Brillouin, La mécanique ondulatoire de Schrödinger: Une méthode générale de resolution par approximations successives, C. R. Acad. Sci. **183**, 23 (1926).

[4] J. B. Keller, Corrected Bohr-Sommerfeld quantum conditions for nonseparable systems, Ann. Phys. (NY) **4**, 180 (1958).

[5] M. Wilkinson, An example of phase holonomy in WKB theory, J. Phys. A: Math. Gen. **17**, 3459 (1984).

[6] K. Yabana and H. Horiuchi, Adiabatic viewpoint for the WKB treatment of coupled channel system: Appearance of the Berry phase and another extra phase accompanying the adiabatic motion, Prog. Theor. Phys. **75**, 592 (1986).

[7] R. G. Littlejohn and W. G. Flynn, Geometric phases in the asymptotic theory of coupled wave equations, Phys. Rev. A **44**, 5239 (1991).

[8] R. G. Littlejohn and W. G. Flynn, Geometric Phases and the Bohr-Sommerfeld Quantization of Multicomponent Wave Fields, Phys. Rev. Lett. **66**, 2839 (1991).

[9] T. Fukui, On the extra phase accompanying Berry's phase in terms of coherent state path integral, Prog. Theor. Phys. **87**, 927 (1992).

[10] K. P. Duncan and B. L. Gy, Semiclassical theory of quasiparticles in the superconducting state, Ann. Phys. (NY) **298**, 273 (2002).

[11] A. Kormányos, P. Rakyta, L. Oroszlány, and J. Cserti, Bound states in inhomogeneous magnetic field in graphene: Semiclassical approach, Phys. Rev. B **78**, 045430 (2008).

[12] T. Tudorovskiy, K. J. A. Reijnders, and M. I. Katsnelson, Chiral tunneling in single and bilayer graphene, Phys. Scr. **T146**, 014010 (2010).

[13] P. Delplace and G. Montambaux, WKB analysis of edge states in graphene in a strong magnetic field, Phys. Rev. B **82**, 205412 (2010).

[14] A. Yu. Ozerin and L. A. Falkovsky, Berry phase, semiclassical quantization, and Landau levels, Phys. Rev. B **85**, 205143 (2012).

[15] Y. Zhang, Y. Barlas, and K. Yang, Coulomb impurity under magnetic field in graphene: A semiclassical approach, Phys. Rev. B **85**, 165423 (2012).

[16] K. J. A. Reijnders, T. Tudorovskiy, and M. I. Katsnelson, Semiclassical theory of potential scattering for massless Dirac fermions, Ann. Phys. (NY) **333**, 155 (2013).

[17] J. Bolte and S. Keppeler, Semiclassical Time Evolution and Trace Formula for Relativistic Spin-1/2 particles, Phys. Rev. Lett. **81**, 1987 (1998).

[18] S. Keppeler, Semiclassical quantisation rules for the dirac and pauli equations, Ann. Phys. (NY) **304**, 40 (2003).

[19] J. Bolte and S. Keppeler, A semiclassical approach to the dirac equation, Ann. Phys. (NY) **274**, 125 (1999).

[20] J. Bolte and R. Glaser, A semiclassical Egorov theorem and quantum ergodicity for matrix valued operators, Commun. Math. Phys. **247**, 391 (2004).

[21] J. Bolte, S. Egger, and S. Keppeler, A Gutzwiller trace formula for large hermitian matrices, arXiv:1512.05984v2.

[22] S. Keppeler, *Spinning Particles: Semiclassics and Spectral Statistics* (Springer, New York, 2003).

[23] P. Carmier and D. Ullmo, Berry phase in graphene: A semiclassical perspective, Phys. Rev. B **77**, 245413 (2008).

[24] J. Dietel and H. Kleinert, Semiclassical approach to the physics of smooth superlattice potentials in graphene, Phys. Rev. B **87**, 235419 (2013).

[25] A. Fasolino, J. H. Los, and M. I. Katsnelson, Intrinsic ripples in graphene, Nat. Mater. **6**, 858 (2007).

[26] J. M. B. Lopes dos Santos, N. M. R. Peres, and A. H. Castro Neto, Graphene Bilayer with a Twist: Electronic Structure, Phys. Rev. Lett. **99**, 256802 (2007).

[27] S. Shallcross, S. Sharma, E. Kandelaki, and O. A. Pankratov, Electronic structure of turbostratic graphene, Phys. Rev. B **81**, 165105 (2010).

[28] S. Shallcross, S. Sharma, and O. Pankratov, Emergent momentum scale, localization, and Van Hove singularities in the graphene twist bilayer, Phys. Rev. B **87**, 245403 (2013).

[29] D. Weckbecker, S. Shallcross, M. Fleischmann, N. Ray, S. Sharma, and O. Pankratov, Low-energy theory for the graphene twist bilayer, Phys. Rev. B **93**, 035452 (2016).

[30] J. S. Alden, A. W. Tsen, P. Y. Huang, R. Hovden, L. Brown, J. Park, D. A. Muller, and P. L. McEuen, Strain solitons and topological defects in bilayer graphene, Proc. Natl. Acad. Sci. USA **110**, 11256 (2013).

[31] B. Butz, C. Dolle, F. Niekiel, K. Weber, D. Waldmann, H. B. Weber, B. Meyer, and E. Spiecker, Dislocations in bilayer graphene, Nature (London) **505**, 533 (2014).

[32] F. Kisslinger, C. Ott, C. Heide, E. Kampert, B. Butz, E. Spiecker, S. Shallcross, and H. B. Weber, Linear magnetoresistance in mosaic-like bilayer graphene, Nat. Phys. **11**, 650 (2015).

[33] J. Wurm, K. Richter, and İ. Adagideli, Edge effects in graphene nanostructures: Semiclassical theory of spectral fluctuations and quantum transport, Phys. Rev. B **84**, 205421 (2011).

[34] C. Emmrich and A. Weinstein, Geometry of the transport equation in multicomponent WKB approximations, Commun. Math. Phys. **176**, 701 (1996).

[35] C. Emmrich and H. Römer, Multicomponent Wentzel-Kramers-Brillouin approximation on arbitrary symplectic manifolds: A star product approach, J. Math. Phys. **39**, 3530 (1998).

[36] P. San-Jose, J. González, and F. Guinea, Non-Abelian Gauge Potentials in Graphene Bilayers, Phys. Rev. Lett. **108**, 216802 (2012).

[37] G. K. MacDonald, E. M. Bennett, P. A. Potter, and N. Ramankutty, Agronomic phosphorus imbalances across the world's croplands, Proc. Natl. Acad. Sci. USA **108**, 3086 (2011).

[38] K. Uchida, S. Furuya, J.-I. Iwata, and A. Oshiyama, Atomic corrugation and electron localization due to moiré patterns in twisted bilayer graphenes, Phys. Rev. B **90**, 155451 (2014).

[39] M. V. Berry and K. E. Mount, Semiclassical approximations in wave mechanics, Rep. Prog. Phys. **35**, 315 (1972).

[40] V. P. Maslov and M. V. Fredoriuk, *Semiclassical Approximation in Quantum Mechanics* (D. Reidel, New York, 1981).

[41] V. P. Maslov, *The Complex WKB Method for Nonlinear Equations I* (Birkhäuser, Basel, 1994).

[42] P. Cvitanovic, R. Artuso, R. Mainieri, G. Tanner, and G. Vattay, Chaos: Classical and Quantum, Niels Bohr Institute, Copenhagen, 2012 (unpublished).

[43] K. G. Budden and M. S. Smith, Phase memory and additional memory in WKB solutions for wave propagation in stratified media, Proc. R. Soc. London, Ser. A **350**, 27 (1976).

[44] M. V. Berry, Budden and Smith's "additional memory" and the geometric phase, Proc. R. Soc. London, Ser. A **431**, 531 (1990).

[45] J. V. José and E. J. Saletan, *Classical Dynamics: A Contemporary Approach* (Cambridge University Press, Cambridge, UK, 1998).

[46] H. Jiang, C.-C. Liu, and Y. Yao, Low-energy effective hamiltonian involving spin-orbit coupling in silicene and two-dimensional germanium and tin, Phys. Rev. B **84**, 195430 (2011).

[47] N. Ray, F. Rost, D. Weckbecker, M. Vogl, S. Sharma, R. Gupta, O. Pankratov, and S. Shallcross, Going beyond k.p theory: A general method for obtaining effective Hamiltonians in both high and low symmetry situations, arXiv:1607.00920.

[48] J. González, Confining and repulsive potentials from effective non-Abelian gauge fields in graphene bilayers, Phys. Rev. B **94**, 165401 (2016).

[49] G. Trambly de Laissardière, D. Mayou, and L. Magaud, Numerical studies of confined states in rotated bilayers of graphene, Phys. Rev. B **86**, 125413 (2012).

[50] W. Landgraf, S. Shallcross, K. Türschmann, D. Weckbecker, and O. Pankratov, Electronic structure of twisted graphene flakes, Phys. Rev. B **87**, 075433 (2013).

[51] K. Richter, Phase coherence effects in antidot lattices: A semiclassical approach to bulk conductivity, Europhys. Lett. **29**, 7 (1995).